From massive MIMO to C-RAN: the OpenAirInterface 5G testbed

Florian Kaltenberger, Xiwen Jiang, Raymond Knopp
EURECOM, Campus SophiaTech, 06410 Biot, France
firstname.lastname@eurecom.fr

***Abstract*—5G will be much more than just a new radio interface - 5G will fundamentally change the way networks are operated. Traditional telecoms equipment will be replaced successively with general purpose computing platforms. This change will affect both the core network and the radio network, where it is also called cloud-RAN (C-RAN). The C-RAN architecture allows for flexible splits between different processing elements in the radio network, for an optimal trade-off between processing in the cloud or in the remote radio unit (RRU).**

OpenAirInterface (OAI) is an open source initiative that today provides Rel-8/Rel-10 3GPP compliant reference implementation of eNodeB, UE, RRH and EPC that runs on general purpose computing platforms. Already today OAI offers several functional splits for its 4G radio stack, for example between the Radio Cloud Center (RCC) and a Remote Radio Unit (RRU). Moreover, Eurecom is currently deploying a C-RAN network at its premises in Sophia-Antipolis, France, using a low-cost solution for RRU based on off-the-shelf equipment.

In this paper we are going to describe the OAI C-RAN architecture with a special emphasis on the possibilities to do multi-cell distributed MIMO processing. In particular we will show how to we can apply our recently developed TDD reciprocity calibration scheme to this distributed setting and integrate it seamlessly into the normal LTE operation.

***Index Terms*—Massive MIMO, TDD, channel reciprocity calibration, distributed antenna system, cloud-RAN, 5G.**

I. Introduction

Wireless networks are evolving from a cellular topology to a cell-free topology, where users are no longer connected to a particular base station, but are served by a large number of distributed antennas. This evolution is supported by two main technologies: massive MIMO and cloud-RAN (C-RAN). Massive MIMO [1], [2] increases spectral efficiency by using a large number of antennas to simultaneously serve multiple users by spatially multiplexing. These antennas can be co-located but also distributed over space. [3] argues that a distributed deployment is able to more efficiently exploit diversity against the shadow fading, and can potentially offer much higher probability of coverage than collocated massive MIMO.

Cloud-RAN technology makes such a distributed antenna processing possible and feasible by centralizing a large part of the physical layer processing on a central server. The C-RAN architecture allows for flexible splits between different processing elements in the radio network, for an optimal trade-off between processing in the cloud or in the remote radio unit. Several such processing splits have been proposed by different communities and standardization bodies [4], [5], [6]. From the perspective of optimizing the spectral efficiency of the system, the lower layer splits are clearly the most promising, since they allow to build a massive MIMO system with a centralized baseband unit and a distributed antenna system based on remote radio heads.

Apart from building such a C-RAN based distributed antenna system, there are also fundamental theoretical problems. In order to make massive MIMO work, channel state information at the transmitter (CSIT) is required. In TDD systems, CSIT can be obtained by exploiting channel reciprocity. However, only the physical channel is reciprocal, while the hardware components such as filters, amplifiers, etc. are not and thus need to be calibrated. Different internal "over the air" calibration methods have been proposed in recent years, such as in [7], [8], [9], [10], [11]. Whereas each method has its pros and cons, it is possible to unify these existing calibration methods under a unified framework [12].

Recently, Eurecom has implemented and demonstrated a massive MIMO TDD testbed that exploits channel reciprocity by calibration [13]. This testbed is based on the Express-MIMO2 software defined radios, a 64-element co-located antenna array, and the OpenAirInterface open-source software radio platform.

In this work we are going to describe the evolution of this testbed to the C-RAN scenario with distributed antenna system. We firstly describe in Section II the current state of the OpenAirInterface software and the cloud-RAN massive MIMO testbed. In Section III we are going to give a brief summary of the generalized reciprocity calibration framework described in [12]. In Section IV we finally describe how we can practically implement the calibration algorithm into the new C-RAN testbed allowing live calibration without disrupting operations. Finally we conclude in Section V.

II. OpenAirInterface and the Eurecom 5G testbeds

OpenAirInterface is an open source initiative that today provides a 3GPP compliant reference implementation of eNodeB (eNB), User Equipment (UE), and evolved packet core (EPC) that runs on general purpose computing platforms together with off-the-shelf software defined radio (SDR) cards like the ETTUS USRP, Lime SDR, and ExpressMIMO2. It allows users to set up a compliant 4G LTE network and inter-operate with commercial equipment.

In this section we firstly describe the "classical" or "monolithic" version of OAI and the existing OAI massive MIMO testbed. Secondly we describe the recently introduced and currently being developed functional splits of OAI that will enable C-RAN deployments of OAI. Last but not leas we describe the current state and vision of the C-RAN testbed at Eurecom and how we are planning to map our existing work on massive MIMO onto this new testbed.

A. Massive MIMO and LTE

Massive MIMO is a hot topic for 5G, but it can also be smartly and perfectly fit into the current LTE standard. In fact, 3GPP has defined the notion of Transmission Modes (TMs) and antenna ports, which can be mapped onto one or more physical antennas. TM 7 is defined in Release 8 and uses antenna port 5 to transmit both data and UE-specific pilots to a single user. The beamforming is thus transparent to the user and can be arbitrary. Release 9 extends TM 7 to TM 8, giving the possibility of transmitting two streams to a single user or two users, whereas in release 10, this is further extended to TM 9 where up to 8 layers for a single user transmission and up to 4 layers for multiuser transmission is supported. Release 11 adds TM 10, similar to TM 9 with up to 8 layers transmission but the transmit antennas can be physically located on different base stations.

OAI currently supports TMs 1,2, and 7, and has experimental versions of TMs 3 and 4. TM 8 and 9 are currently in development. OAI does not (yet) support any CSI reference signals, but it does support sounding reference signal (SRS), which can be used in TDD together with a proper reciprocity calibration mechanism to estimate the CSIT.

The Eurecom massive MIMO testbed is based on TDD and TM 7 driving up to 64 co-located antenna elements. It uses uplink channel estimates based on the SRS and transforms them with the help of the calibration matrix (see next section) to a downlink channel estimate, which is then used to compute the beamforming weights. During our experiments we were able to establish communication with a commercial UE and achieve the maximum possible throughput for the given configuration [13].

B. Functional splits in OAI

In the massive MIMO testbed described above, all the eNB functionality was running in the same machine (using heavy parallelization to meet the real-time constraints). In order to support a distributed antenna array built from remote radio heads, the monolithic architecture of OAI is split into several parts.

We have adopted the definitions of [4] for the software architecture of OAI. The eNB protocol stack is split in 3 different parts: the remote radio unit (RRU), which is an evolution of the classical remote radio head (RRH), the radio aggregation unit (RAU), which controls multiple RRUs potentially operating on different bands and with different coverages. As the name suggests this unit is responsible also for carrier aggregation and in the future also different radio access technologies. Last

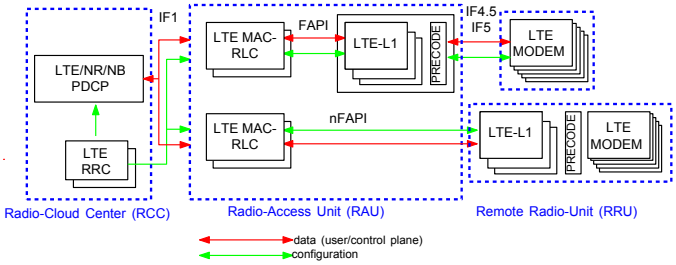

Fig. 1. OAI functional splits

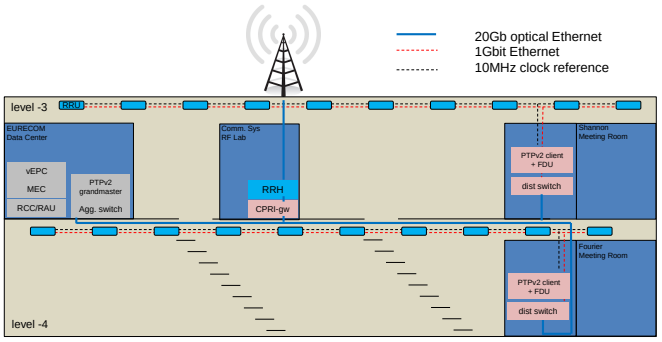

Fig. 2. Floor plan of the Eurecom C-RAN deployment

but not least the Radio Cloud Center (RCC) controls multiple RAUs. In the 3GPP 5G specifications the RCC is also called the central unit (CU) and RAU the distributed unit (DU).

The split between RRU and RAU is flexible and there are three possible options in OAI. IF5 is similar to the classical BBU-RRH interface and transports baseband time domain IQ samples. IF4.5 corresponds to the split-point at the input (TX) and output (RX) of the OFDM symbol generator (i.e., frequency-domain signals) and transports resource elements in the usable channel band. Both interfaces also support optional A-law compression. Additionally to these two interfaces, OAI today also supports the small cells FAPI interface specifications P5 and P7 between the PHY and the MAC layer [14] that allows to offload the lower PHY functionality to the RRU.

The interface between RAU and RCC is currently under development and we are retro-fitting the current 5G-NR specifications [15] for the F1 interface between CU and DU to 4G.

C. C-RAN testbed

Eurecom is currently building and deploying a C-RAN network on its premises in Sophia-Antipolis. The platform will consist of a set of RRUs deployed on the ceilings of the corridors on levels -3 and -4 of the EURECOM building. The RRUs on each floor are connected by Gbit Ethernet to a switch which are in turn connected to a central server over optical 20Gbit Ethernet. An additional high power commercial remote radio head is connected to the C-RAN server through a CPRI gateway (see Figure 2).

Frequency synchronization is provided by a clock distribution unit which provides a 10MHz reference signal on each

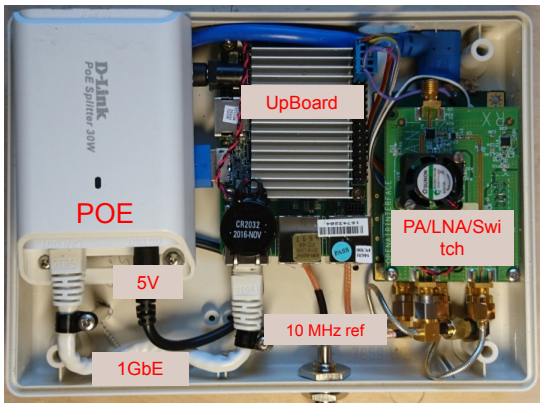

Fig. 3. Remote Radio Unit (RRU) built from commodity hardware

floor. Timing synchronization is achieved by a special protocol in the RRUs that first listens to other RRUs within its range to derive the frame number and the start of the frame. In the future, the FDUs on each floor can further be synchronized using the PTPv2 (IEEE 1588) protocol over optical fiber. For this a PTPv2 grandmaster clock will be placed in the server room and a PTPv2 client in the local server rooms.

The RRUs consist of an up-board from Intel, a B200 mini from Ettus research, a RF frontend designed by Eurecom and PoE module (see Figure 3). The RRUs will use Band 38 (2.5 GHz) time-division duplex (TDD) for which EURECOM has been granted a license from the French regulatory body (ARCEP) for both indoor and short-range outdoor experiments (1km radio around our building).

III. Over-the-air reciprocity calibration framework

As mentioned in the introduction, calibration is necessary to exploit reciprocity in TDD systems. In this section we review our mathematical framework for reciprocity calibration from [12] while in the next section we explain how we will apply this method to our C-RAN testbed.

A. Reciprocity calibration

Consider a system in Fig. 4, where A is a BS and B is a UE, each containing M_A and M_B antennas. The DL and UL channel (in frequency domain) seen in the digital domain can be represented by

$$\begin{cases} \mathbf{H}_{A\to B} = \mathbf{R}_B \mathbf{C}_{A\to B} \mathbf{T}_A \\ \mathbf{H}_{B\to A} = \mathbf{R}_A \mathbf{C}_{B\to A} \mathbf{T}_B, \end{cases} \tag{1}$$

where $\mathbf{T}_A$, $\mathbf{R}_A$, $\mathbf{T}_B$, $\mathbf{R}_B$ represent the transmit and receive RF front-ends for BS and UE respectively. The size of $\mathbf{T}_A$ and $\mathbf{R}_A$ are $M_A \times M_A$, whereas that of $\mathbf{T}_B$ and $\mathbf{R}_B$ are $M_B \times M_B$. These matrices are usually diagonal since the off-diagonal elements corresponding to RF crosstalk and antenna mutual coupling are usually very small.

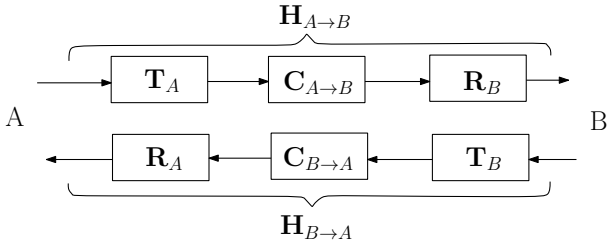

Fig. 4. Reciprocity model.

As the system is operating under TDD mode, within the channel coherence time, $\mathbf{C}_{A\to B} = \mathbf{C}_{B\to A}^T$, we can easily obtain the relationship of the bi-directional channels:

$$\mathbf{H}_{A\to B} = \mathbf{F}_B^{-T} \mathbf{H}_{B\to A}^T \mathbf{F}_A. \tag{2}$$

where diagonal matrices $\mathbf{F}_A = \mathbf{R}_A^{-T}\mathbf{T}_A$ and $\mathbf{F}_B = \mathbf{R}_B^{-T}\mathbf{T}_B$ are named calibration matrices.

A TDD reciprocity based MIMO system usually performs reciprocity calibration in order to estimate $\mathbf{F}_A$ and $\mathbf{F}_B$. Then for data transmission, they are used together with instantaneous measured UL channel $\hat{\mathbf{H}}_{B\to A}$ to estimate the CSIT $\mathbf{H}_{A\to B}$, based on which advanced beamforming algorithms can be performed. Since the calibration coefficients stay stable during quite a long time [7], the calibration process doesn't have to be done very frequently.

Among existing calibration methods in literature, BS internal "over the air" calibration attracts most attention and thus is used in the OpenAirInterface massive MIMO and C-RAN testbed. "Over the air" calibration replies on pilot exchange and signal processing, which differs with calibration using additional hardware, and appears more cost effective. By "BS internal" calibration, we refer to methods without the involvement of terminals (no feedback from UE is needed), i.e., only $\mathbf{F}_A$ is estimated, whereas $\mathbf{F}_B$ is taken as an identity matrix. Thus all the calibration process is performed internally at the BS antenna array. In fact, previous studies in [16], [17] pointed out that the impact of hardware asymmetry on the BS side has a much more severe impact on the beamforming performance than on the UE side.

B. "Over the air" calibration framework

Different "over the air" calibration methods can be unified under a general framework. Let us concentrate on BS internal calibration (although the framework is not limited to this case) and consider an antenna array of M elements partitioned into G groups denoted by $A_1, A_2, \ldots, A_G$, as in Fig. 5, where group A_i contains M_i antennas such that $\sum_{i=1}^{G} M_i = M$. Each group A_i transmits a sequence of L_i pilot symbols, defined by matrix $\mathbf{P}_i \in \mathbb{C}^{M_i \times L_i}$ where the rows correspond to antennas and the columns to successive channel uses. A channel use can be understood as a time slot or a sub-carrier in an OFDM-based system. The bidirectional transmission between antenna groups i and j is given by

$$\begin{cases} \mathbf{Y}_{i\to j} = \mathbf{R}_j \mathbf{C}_{i\to j} \mathbf{T}_i \mathbf{P}_i + \mathbf{N}_{i\to j} \\ \mathbf{Y}_{j\to i} = \mathbf{R}_i \mathbf{C}_{j\to i} \mathbf{T}_j \mathbf{P}_j + \mathbf{N}_{j\to i} \end{cases} \tag{3}$$

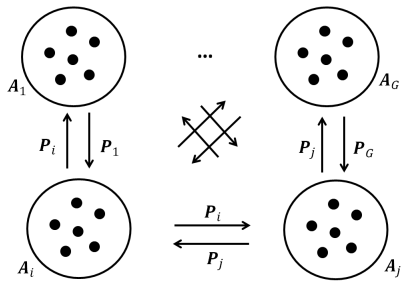

Fig. 5. Bi-directional transmission between antenna groups.

where $\mathbf{Y}_{i\to j}$ and $\mathbf{Y}_{j\to i}$ are received signal at antenna groups j and i respectively when the other group is transmitting. $\mathbf{N}_{i\to j}$ and $\mathbf{N}_{j\to i}$ represent the corresponding received noise matrix. $\mathbf{T}_i$ and $\mathbf{T}_j$ represent RF front-ends properties. The reciprocity property induces that $\mathbf{C}_{i\to j} = \mathbf{C}_{j\to i}^T$, thus for two different groups $1 \le i \ne j \le G$ in (3), by eliminating $\mathbf{C}_{i\to j}$ we have,

$$\mathbf{P}_i^T \mathbf{F}_i^T \mathbf{Y}_{j\to i} - \mathbf{Y}_{i\to j}^T \mathbf{F}_j \mathbf{P}_j = \widetilde{\mathbf{N}}_{ij}, \tag{4}$$

where the noise component $\widetilde{\mathbf{N}}_{ij} = \mathbf{P}_i^T \mathbf{F}_i^T \mathbf{N}_{j\to i} - \mathbf{N}_{i\to j}^T \mathbf{F}_j \mathbf{P}_j$, while $\mathbf{F}_i = \mathbf{R}_i^{-T} \mathbf{T}_i$ and $\mathbf{F}_j = \mathbf{R}_j^{-T} \mathbf{T}_j$ are the calibration matrices for groups i and j. The whole calibration matrix $\mathbf{F}$ is diagonal, and thus takes the form of $\mathbf{F} = \text{diag}\{\mathbf{F}_1, \mathbf{F}_2, \ldots, \mathbf{F}_G\}$.

Let us use $\mathbf{f}_i$ and $\mathbf{f}$ to denote the vectors of the diagonal coefficients of $\mathbf{F}_i$ and $\mathbf{F}$ respectively, i.e., $\mathbf{F}_i = \text{diag}\{\mathbf{f}_i\}$ and $\mathbf{F} = \text{diag}\{\mathbf{f}\}$. This allows us to vectorize (4) into

$$(\mathbf{Y}_{j\to i}^T * \mathbf{P}_i^T)\mathbf{f}_i - (\mathbf{P}_j^T * \mathbf{Y}_{i\to j}^T)\mathbf{f}_j = \widetilde{\mathbf{n}}_{ij}, \tag{5}$$

where $*$ denotes the Khatri–Rao product (or column-wise Kronecker product), where we have used the equality $\text{vec}(\mathbf{A}\,\text{diag}(\mathbf{x})\,\mathbf{B}) = (\mathbf{B}^T * \mathbf{A})\,\mathbf{x}$. Finally, stacking equations (5) for all $1 \le i < j \le G$ yields

$$\boldsymbol{\mathcal{Y}}(\mathbf{P})\mathbf{f} = \widetilde{\mathbf{n}} \tag{6}$$

with $\boldsymbol{\mathcal{Y}}(\mathbf{P})$ defined as

$$\underbrace{\begin{bmatrix} (\mathbf{Y}_{2\to 1}^T * \mathbf{P}_1^T) & -(\mathbf{P}_2^T * \mathbf{Y}_{1\to 2}^T) & 0 & \cdots \\ (\mathbf{Y}_{3\to 1}^T * \mathbf{P}_1^T) & 0 & -(\mathbf{P}_3^T * \mathbf{Y}_{1\to 3}^T) & \cdots \\ 0 & (\mathbf{Y}_{3\to 2}^T * \mathbf{P}_2^T) & -(\mathbf{P}_3^T * \mathbf{Y}_{2\to 3}^T) & \cdots \\ \vdots & \vdots & \vdots & \ddots \end{bmatrix}}_{(\sum_{j=2}^{G}\sum_{i=1}^{j-1} L_i L_j)\times M}. \tag{7}$$

A typical way to estimate the calibration parameters $\mathbf{f}$ consists in solving a Least square (LS) problem such as

$$\hat{\mathbf{f}} \;=\; \arg\min \|\boldsymbol{\mathcal{Y}}(\mathbf{P})\,\mathbf{f}\|^2 \tag{8}$$

where $\boldsymbol{\mathcal{Y}}(\mathbf{P})$ is defined in (7). If we assume $\mathbf{e}_1^H \mathbf{f} = 1$, The solution of (8) is given by

$$\hat{\mathbf{f}} \;=\; \frac{1}{\mathbf{e}_1^H (\boldsymbol{\mathcal{Y}}(\mathbf{P})^H \boldsymbol{\mathcal{Y}}(\mathbf{P}))^{-1} \mathbf{e}_1} (\boldsymbol{\mathcal{Y}}(\mathbf{P})^H \boldsymbol{\mathcal{Y}}(\mathbf{P}))^{-1} \mathbf{e}_1. \tag{9}$$

Assuming a unit norm constraint on the other hand yields

$$\hat{\mathbf{f}} = V_{min}(\boldsymbol{\mathcal{Y}}(\mathbf{P})^H \boldsymbol{\mathcal{Y}}(\mathbf{P})) \tag{10}$$

where $V_{min}(\mathbf{X})$ denotes the eigenvector of matrix $\mathbf{X}$ corresponding to its eigenvalue with the smallest magnitude. Note that the proposed framework also allows to consider using only subsets of the received data which corresponds to some of the methods found in the literature.

Antenna partition offers a framework generalizing existing reciprocity calibration methods. For example, if we partition the array into a reference antenna and a group containing all other antennas, performing bi-directional transmission using timely orthogonal pilots, leads to the Argos calibration method in [7]. The LS method [8] consists in defining groups each with one antenna, whereas a full Avalanche calibration [9] is equivalent to partition the antenna array into groups with $\max\{1, i-1\}$ where i is the index of the antenna group.

IV. Reciprocity calibration in OpenAirInterface C-RAN testbed

In order to keep the OpenAirInterface C-RAN testbed in a calibrated status, reciprocity calibration should be performed online, without interrupting data streaming. The most suitable place to carry out calibration is thus the special subframe in a TDD frame, where we can take use of several OFDM systems to perform pilot transmission between different RRUs. The principle is shown in Fig. 6, where at each special subframe every 10ms (TDD configuration 3 is considered), two RRUs are selected with one transmitting the other RRU listening. In order to have enough time for the hardware to switch from transmit (Tx) mode to receive (Rx) mode, we reserve 3 OFDM symbol duration as the transition period. The transmitting RRU starts to switch from Tx to Rx at symbol 9 whereas the listening RRU start to switch from Tx to Rx mode at symbol 1 (only one PDCCH symbol is transmitted in the DL, whereas PSS is sacrificed). By differentiating the switching time, we have 5 OFDM symbol duration to transmit calibration pilot from the transmitting RRU to the listening RRU. In the coming special subframe of the next frame, we switch the role of transmitting and listening RRUs, thus collect a bi-direction pilot exchange for a pair of RRUs every 20ms. The system then goes through all pairs of RRUs (with good enough channels) a round robin manner. If all pairs of RRUs in the distributed radio system have good enough channels between them, we need $M(M-1)\times 10$ms to collect all bi-directional observations for calibration estimation. We point here that, in order to have least inference during pilot transmission in the subframe, the other $M-1$ RRUs can start to switch from Tx to Rx in the same way as the listening RRU[1].

From system implementation point of view, the easiest way to transmit pilot and collect observations between RRUs is to reuse the cell specific reference signals (RSs) in symbol 4 and 7. The bi-directional pilot exchange between two RRUs has to

[1]If the channel coherence time is large enough, reciprocity calibration can also be carried out in a way that at each special subframe, only one RRU is transmitting and all other RRUs are listening, we then let each RRU take the role as a transmitting RRU in a round robin manner, and use all received observations from the other RRUs to estimate calibration coefficients. In this mode, only $M \times 10$ms are needed to collect all observations.

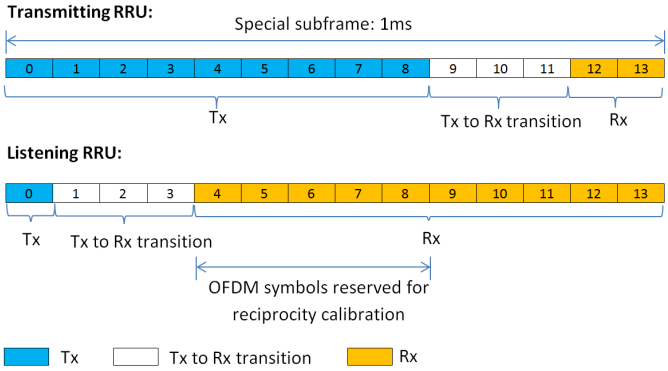

Fig. 6. Transmit to receive mode switch on transmitting and listening RRU in special subframe.

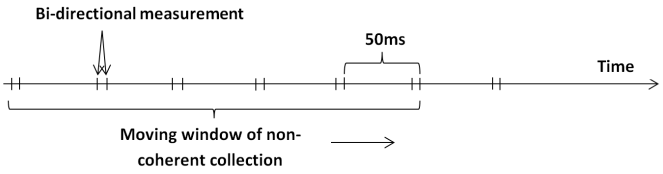

Fig. 7. Collection of observation for each pair of RRUs every 50ms.

be happen in two consecutive frames, however, for different pairs of RRU, the collection does not have to be done in a intensive manner. it is possible to collect observations for a pair of observation, e.g., every 50ms, as in Fig. 7. We then use a moving window that contain all recent collected observations for calibration. Each time a new pair of observation comes into the windows the corresponding old observation is abandoned. We thus keep updating the calibration coefficients which can suffer some small smooth variations due to environmental factors, such as temperature.

In the current C-RAN setup, each RRU has only one antenna, which corresponds to the case of single antenna grouping in our framework described in Section III-B. Estimating calibration coefficients using (9) and (10) can take a considerable calculation resources, however is not too much constrained by real time processing. This task can be performed in the cloud where complexity optimized algorithms are under development. When the system is streaming data to UEs, instantaneously estimated UL channels are then used together with calculated calibration coefficients to estimate DL CSIT and beamforming weights. The central controller (RRC) then sends the beamforming weights to each RAU to perform beamforming precoding whereas the precoded OFDM symbols are then transmitted to RRU through IF4.5.

V. Conclusions

Massive MIMO is not just a hype anymore, but is being integrated and deployed in commercial systems, where it is mainly used for high (above 6GHz) frequencies and co-located antenna deployments to overcome the difficult propagation conditions there. At lower frequencies, the size of the antennas make it difficult to build very large co-located MIMO systems. Here, distributed massive MIMO are a promising solution. However, current state-of-the art equipment using remote radio heads connected to a centralized base-band over CPRI or other standards is a very expensive solution. In this paper we have presented a cheap alternative solution that relies on (1) commodity computing and radio components to build remote radio unit, and (2) a flexible interface between the RRU and the RAU implemented using cheap Gbit Ethernet connections and a clock distribution unit. Moreover we have shown how to exploit channel reciprocity in such a distributed massive MIMO system and integrate the calibration into the normal LTE TDD operation.

References

[1] T. Marzetta, "Noncooperative cellular wireless with unlimited numbers of base station antennas," *IEEE Trans. Wireless Commun.*, vol. 9, no. 11, pp. 3590–3600, Nov. 2010.

[2] E. Larsson, O. Edfors, F. Tufvesson, and T. Marzetta, "Massive MIMO for next generation wireless systems," *IEEE Commun. Mag.*, vol. 52, no. 2, pp. 186–195, Feb. 2014.

[3] H. Q. Ngo, A. Ashikhmin, H. Yang, E. G. Larsson, and T. L. Marzetta, "Cell-free massive mimo versus small cells," *IEEE Transactions on Wireless Communications*, vol. 16, no. 3, pp. 1834–1850, March 2017.

[4] China Mobile, Alcatel-Lucent, Nokia Networks, ZTE Cooperation, Broadcom Cooperation, and Intel China, "Next generation fronthaul interface," White paper, Jun. 2015. [Online]. Available: http://labs.chinamobile.com/cran/2015/09/29/white-paper-of-ngfinext-generation-fronthaul-interface-version-1-0en/

[5] IEEE, "P1914.1 standard for packet-based fronthaul transport networks," 2017. [Online]. Available: http://sites.ieee.org/sagroups-1914/

[6] 3GPP, "Radio access architecture and interfaces," 3GPP, Tech. Rep. 38.801, Mar. 2017.

[7] C. Shepard, H. Yu, N. Anand, E. Li, T. Marzetta, R. Yang, and L. Zhong, "Argos: Practical many-antenna base stations," in *Proc. ACM Intern. Conf. Mobile Computing and Netw. (Mobicom)*, Istanbul, Turkey, Aug. 2012, pp. 53–64.

[8] R. Rogalin, O. Bursalioglu, H. Papadopoulos, G. Caire, A. Molisch, A. Michaloliakos, V. Balan, and K. Psounis, "Scalable synchronization and reciprocity calibration for distributed multiuser MIMO," *IEEE Trans. Wireless Commu.*, vol. 13, no. 4, pp. 1815–1831, Apr. 2014.

[9] H. Papadopoulos, O. Y. Bursalioglu, and G. Caire, "Avalanche: Fast RF calibration of massive arrays," in *Proc. IEEE Global Conf. on Signal and Information Process. (GlobalSIP)*, Washington, DC, USA, Dec. 2014, pp. 607–611.

[10] H. Wei, D. Wang, H. Zhu, J. Wang, S. Sun, and X. You, "Mutual coupling calibration for multiuser massive MIMO systems," *IEEE Trans. on Wireless Commun.*, vol. 15, no. 1, pp. 606–619, 2016.

[11] J. Vieira, F. Rusek, O. Edfors, S. Malkowsky, L. Liu, and F. Tufvesson, "Reciprocity calibration for massive MIMO: Proposal, modeling, and validation," *IEEE Trans. on Wireless Comm.*, vol. 16, no. 5, pp. 3042–3056, 2017.

[12] X. Jiang, A. Decunringe, K. Gopala, F. Kaltenberger, M. Guillaud, D. Slock, and L. Deneire, "A framework for over-the-air reciprocity calibration for tdd massive MIMO systems," *IEEE Trans. on Wireless Communications*, 2017, submitted. [Online]. Available: http://arxiv.org/abs/1710.10830

[13] X. Jiang and F. Kaltenberger, "Demo: an LTE compatible massive MIMO testbed based on openairinterface," in *WSA 2017; 21th International ITG Workshop on Smart Antennas*, March 2017, pp. 1–2.

[14] Small Cell Forum, "FAPI and nFAPI specifications," Small Cell Forum, Tech. Rep. 082.09.05, May 2017.

[15] 3GPP, "F1 general aspects and principles," 3GPP, Technical specifcation 38.470, Sep. 2017.

[16] Huawei, "Hardware calibration requirement for dual layer beamforming," 3GPP RAN1 #57, 3GPP, San Francisco, USA, Tech. Rep. R1-091794, May 2009.

[17] Nokia, Nokia Siemens Networks, CATT, and ZTE, "Performance study on Tx/Rx mismatch in LTE TDD dual-layer beamforming," 3GPP RAN1 #57, 3GPP, San Francisco, USA, Tech. Rep. R1-091752, May 2009.